ROYAL SOCIETY OF CHEMISTRY

PAPER

Check for updates

Reactivity of phenoxathiin-based thiacalixarenes towards *C*-nucleophiles†‡

Kamil Mamleev,[a] Jan Čejka, [ID][b] Václav Eigner, [ID][b] Martin Krupička,[a] Hana Dvořáková [ID][c] and Pavel Lhoták [ID]*[a]

A starting thiacalix[4]arene can be easily transformed into oxidized phenoxathiin-based macrocycles **9** and **9'**, representing an unusual structural motif in calixarene chemistry. The presence of electron-withdrawing groups (SO₂, SO) and the considerable internal strain caused by the condensed heterocyclic moiety render these molecules susceptible to nucleophilic attack. The reaction with various organolithium reagents provides a number of different products resulting from the cleavage of either the calixarene skeleton or the phenoxathiin group or both ways simultaneously. This enables the preparation of thiacalixarene analogues with unusual structural features, including systems containing a biphenyl fragment as a part of the macrocyclic skeleton. The above-described transformations, unparalleled in classical calixarene chemistry, clearly demonstrate the synthetic potential of this thiacalixarene subgroup.
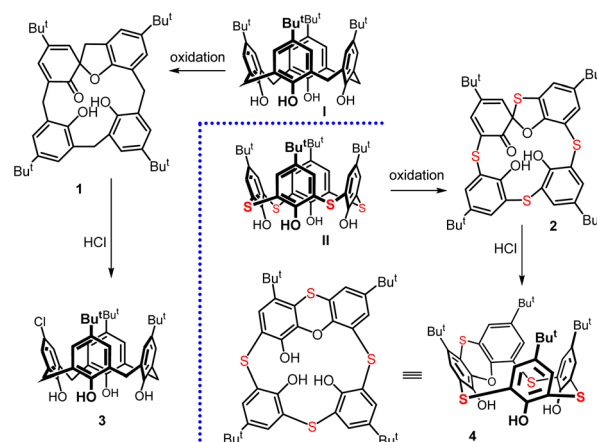
Introduction

Thiacalixarenes[1] are sulfur analogues of classical calixarenes[2] and have similar uses in supramolecular chemistry to a large extent. However, the presence of sulfurs instead of CH₂ bridges brings several new properties that were not known in the original macrocycles.[3] For example, chemoselective oxidation of sulfur (sulfone *vs.* sulfoxide) can lead to a whole other series of building blocks, where regio- or stereo-selective reactions often result in inherently chiral systems.[4] Thia analogues can differ in conformational preferences and their cation complexation abilities.[5]

There are interesting differences in the subsequent derivatization of these two systems. The introduction of sulfur significantly alters the macrocycle's reactivity. This can be demonstrated in the example of the so-called spirodienones,[6] originally known from classical calixarenes chemistry, where they were utilized to obtain the substitution patterns that would have been challenging to access otherwise.[7] These compounds **1** and **2** (Scheme 1) can be produced in high yields by the oxidation of the starting macrocycles **I** and **II** with chloramine-T. The

CH₂ analogue **1** is transformed into the monochlorinated calix[4]arene **3** by the reaction with HCl.[8] In contrast, the thiaderivative **2** (ref. 9) provides a completely different type of chemistry and its reaction with HCl leads (virtually quantitatively) to the rearranged structure **4** bearing a phenoxathiin moiety (Scheme 1).[10]

Macrocycle **4** has possible applications in chiral recognition due to its inherently chiral structure.[11] In addition, we recently found that the oxidized form[12] of this compound, which bears a sulfoxide group on the phenoxathiin moiety, displays unexpected stereochemical preferences of the sulfoxide during the transformations.[13] Furthermore, compound **5** demonstrates an uncommon reactivity with specific nucleophiles, as shown in

ªDepartment of Organic Chemistry, University of Chemistry and Technology, Prague (UCTP), Technicka 5, 166 28 Prague 6, Czech Republic. E-mail: lhotakp@vscht.cz; Fax: +420-220444288; Tel: +420-220445055
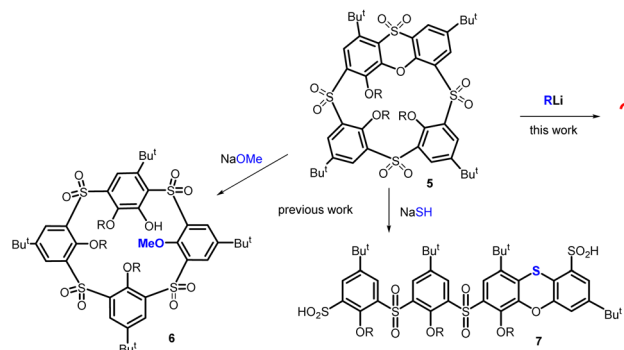
ᵇDepartment of Solid State Chemistry, UCTP, 166 28 Prague 6, Czech Republic

ᶜLaboratory of NMR Spectroscopy, UCTP, 166 28 Prague 6, Czech Republic

Scheme 1 The formation of spirodienone derivatives (**1** and **2**) and their different reactivity towards hydrochloric acid – formation of **3** and **4**, respectively.

Scheme 2 Cleavage of the phenoxathiin moiety by different nucleophiles.

Scheme 2. A reaction with *O*-nucleophiles (*e.g.* MeO⁻) cleaves the phenoxathiin system, forming macrocycle **6** that possesses features of both pillararenes (*para*-bridge) and calixarenes (*meta*-bridge).[14]

Interestingly, the reaction with *S*-nucleophile (NaSH) yields the unexpected linear tetramer bis-sulfinic acid **7** with a rearranged phenoxathiin moiety.[15] The complex reaction pathway proceeds *via* a unique cascade of three consecutive SₙAr steps triggered by the initial attack of the SH⁻ nucleophile.

In this article, we report on the unforeseen reactivity of macrocycle **5** towards the *C*-nucleophiles, specifically with organolithium reagents. The macrocycle and/or the phenoxathiin core can be split depending on the reagent used and the reaction conditions. This cleavage results in the formation of a whole range of linear and macrocyclic derivatives. The macrocycles exhibit unique structural features not previously described in calixarenes/thiacalixarenes chemistry. Therefore, these derivatives offer novel alternative types of macrocycles that can be used in supramolecular chemistry.

Results and discussion

The oxidized phenoxathiin-based thiacalix[4]arenes **9** and **9′** were synthesized according to published procedures[12] as shown
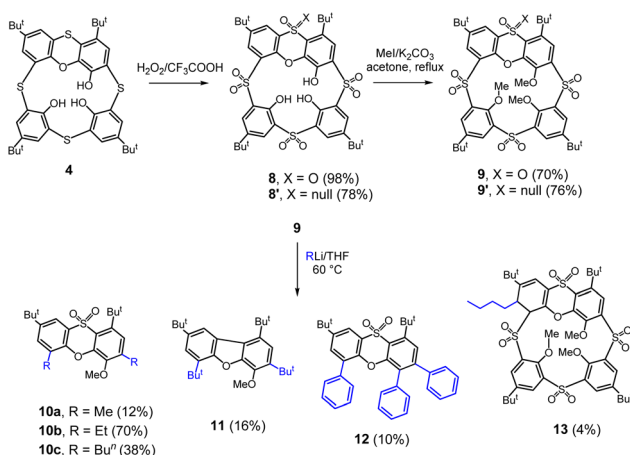
Scheme 3 Cleavage of compound **9** with organolithium compounds.

in Scheme 3. The starting phenoxathiin **4** (obtained from thiacalix[4]arene **II** using procedure[10] described in the literature) was oxidized with an excess of 30% aq. H₂O₂ in TFA/CHCl₃ (4 days reflux) to provide the corresponding crude sulfone[12] **8** in a 98% yield (Scheme 3). Sulfoxide **8′** was obtained as the sole product chemoselectively in a 78% yield after performing the reaction overnight in the dark at room temperature.[13] Both isomers **8** and **8′** were then reacted without further purification with MeI in the presence of Cs₂CO₃ as a base (reflux in acetone) to produce the alkylated[12] macrocycles **9** and **9′** in 70 and 76% overall yields (from **4**), respectively.

In our previous study, we reported that the phenoxathiin moiety of **9** can be cleaved by alkoxides, generating a new type of macrocycle[14] **6** (Scheme 2). However, a similar reaction with NaSH led to a cascade of three successive SₙAr steps resulting in the opening of the macrocycle accompanied by the rearrangement[15] of phenoxathiin moiety (compound **7**, Scheme 2). To investigate the reactivity towards the *C*-nucleophiles, sulfone **9** in THF was reacted with several different types, including NaCN, Grignard reagents and organolithium compounds. To our surprise, only the organolithium reagents showed some reactivity at room temperature but with a very low conversion of the starting compound. Increasing the reaction temperature and using an excess of alkyllithium eventually caused the complete disappearance of the starting material and the formation of the product. Hence, a reaction of **9** with 6 equivs. of EtLi at 60 °C for 1 h gave 70% of the product assigned as **10b** (Scheme 3). The ¹H NMR spectrum (DMSO-d_6, 400 MHz) showed two doublets (7.81 and 7.78 ppm) in the aromatic region with typical *meta* coupling constants ($J = 2.5$ Hz) and a singlet at 7.40 ppm. The presence of two *tert*-butyl groups (1.37 and 1.61 ppm) and two different ethyl groups in the aliphatic part of the spectrum indicated the break of the macrocycle upon entering two organolithium reagents into the molecule. The molecular mass found in the HRMS (ESI⁺) spectrum ($m/z = 431.2250$) also precisely agreed with the expected value [M + H]⁺ for **10b** (C₂₅H₃₄O₄S).

The single crystal X-ray analysis unambiguously proved the structure. It revealed that **10b** crystallized in a monoclinic system, a space group $P2_1/n$. The molecule retains its phenoxathiin skeleton, but with two added ethyl groups replacing the original –SO₂– bridges (Fig. 1a). The phenoxathiin moiety is nonplanar and the two outer benzene rings form an angle of 130.16° (Fig. 1b). Because of its curvature, compound **10b** is inherently chiral and both enantiomers are found within the unit cell as a racemic mixture.

Similar products **10a** and **10c** were also isolated using MeLi and *n*-BuLi agents, respectively. As illustrated in Scheme 4, these compounds are produced by the attack of an organolithium reagent on the phenoxathiin group at the point of attachment of the sulfonyl bridge. This is followed by the elimination of the sulfinic acid, which acts as a leaving group, thus representing a nucleophilic aromatic substitution SₙAr reaction. The addition of organolithium agent is facilitated by the presence of another electron-withdrawing group (SO₂) on the same aromatic moiety. A similar reactivity was described *e.g.* for derivatives of 2-(phenylsulfonyl)-1,3-oxazole[16] where sulfonyl
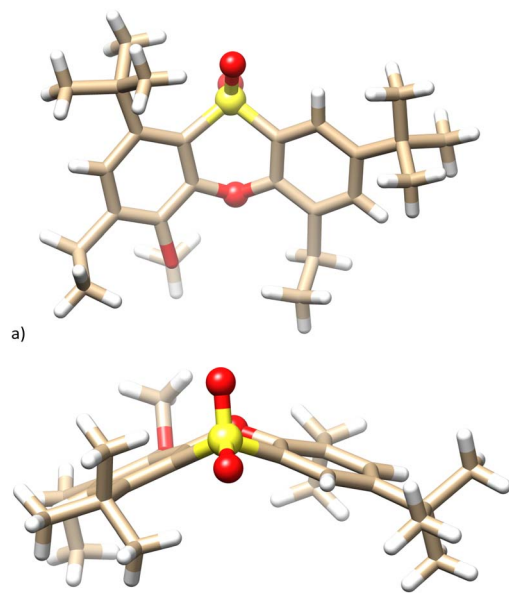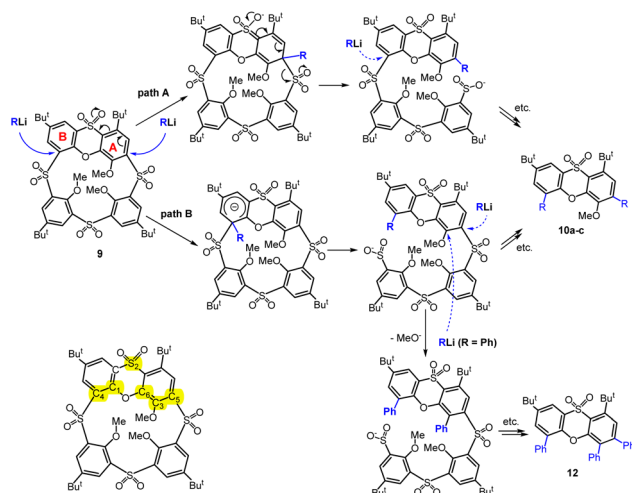
Fig. 1 Single crystal X-ray structure of the compound **10b**. (a) Side view; (b) top view; heteroatoms in phenoxathiin moiety shown as balls for better clarity.

Scheme 4 Nucleophilic aromatic substitution of $-SO_2-$ bridges in the phenoxathiin moiety; numbering used in Table 1.

moiety was displaced by several organolithium reagents in good yields.

Technically speaking, the phenoxathiin moiety can be attacked first at the A subunit (where the sulfone group in the *p*-position should assist), and then a similar attack can occur at the B subunit to form the product (path A, Scheme 4). The second alternative is the reverse order, where the B moiety would react first, and only then A is attacked (path B, Scheme 4).

We tried to explore the reactivity of **9** using computational chemistry methods. The isolated products shown in Scheme 3 can be obtained *via* various pathways and we therefore concentrated only on the barriers of the first step – addition of

the organolithium compound. The sites of possible nucleophilic attacks at phenoxathiin moiety are shown in Scheme 4, and we compared the activation energies for the addition of PhLi and MeLi to the macrocyclic skeleton (see Table 1). During reaction, the lithium atom from the organolithium reagent becomes stabilized by the interactions with the neighbouring SO_2 group and the oxygen atom of the phenoxathiin moiety – see Fig. 2 for the transition state structures. The possibility of Li^+ stabilization is probably another important factor for regioselectivity, together with the preference for stabilization of the emerging anionic intermediate, similar to Meisenheimer complex.

The calculations showed that the most favourable attack site is the C_4 in unite B, which leads to opening of the macrocyclic skeleton, thus corresponding to the reaction path B (Scheme 4). The subsequent fate of the molecule is difficult to ascertain, as the geometry of the molecule changes, although the electronic effects remain essentially the same. The relative activation energies $\Delta\Delta E^{\ddagger}$ are reported in Table 1. As can be seen, the order of reactivity is the same for both reagents (MeLi and PhLi) and the attack on the aromatic nucleus B takes place preferentially. The difference in $\Delta E^{\ddagger}$ compared to the attack on the nucleus A (position C5) is more than 6.9 and 10.8 kcal mol^{-1}, respectively. The structures of the corresponding transition states for MeLi and PhLi can be seen in Fig. 2.

The unpredicted product **12** was identified in a reaction with phenyllithium (Scheme 3). The ^{1}H NMR spectrum (CDCl$_3$, 400 MHz) did not show methoxy group, however, it displayed three distinct phenyl moieties, suggesting that the MeO group was replaced with an additional phenyl group.[18] The molecular peak at $m/z = 595.2280$ in the HRMS ESI$^+$ spectrum confirmed this assumption (compare $m/z = 595.2277$ calc. for [**12**+Na]$^+$). Considering the SO_2 bond cleavage mechanism mentioned above, it is probable that the methoxy group substitution occurs before the final cleavage of the macrocycle, due to the stabilizing effect of the neighbour sulfone bridge (see Scheme 4).

The X-ray analysis confirmed the proposed structure. Compound **12** crystallised in a monoclinic system, a space group $P2_1/c$. The phenoxathiin skeleton exhibits structural features very similar to compound **10b**. An additional phenyl is responsible for a significant twisting of the phenyl substituents

Table 1 The comparison of relative activation energy^a (relative to free reactants) for the first addition step (see Scheme 4) of organolithium agent to the phenoxathiine moiety of compound **9**^{b}

Position	$\Delta\Delta E^{\ddagger}$ [kcal mol^{-1}]	
	MeLi	PhLi
C1	8.40	8.40
S2	17.62	17.20
C3	7.89	8.24
C4	0.00	0.00
C5	6.90	10.80
C6	15.80	14.48

^{a} The lowest activation energy is set to zero. ^{b} Obtained by the GFN2-XTB method.[17]
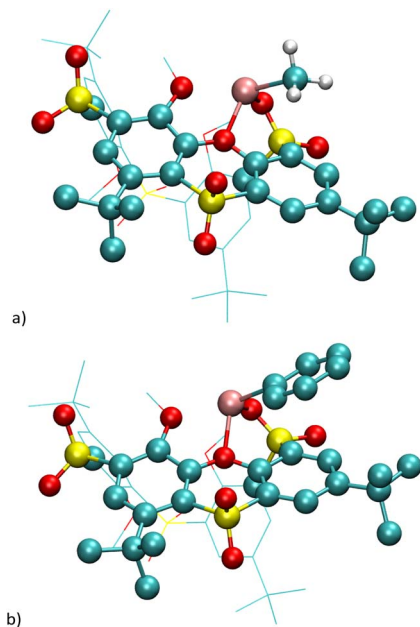
Fig. 2 Structures of the transition state of the first reaction step: **9** + RLi: (a) addition of MeLi (path B, Scheme 4); (b) addition of PhLi (path B, Scheme 4).

out of the plane of phenoxathiine benzene rings. As depicted in Fig. 2a, the corresponding interplanar angles (biphenyl-like substructures) are 48.66° (blue), 61.60° (violet) and 52.52° (shadow). The twisted non-planar structure enables the formation of a dimer composed of both enantiomers in the solid phase, where several CH–π and π–π interactions (T-shaped) can be found (see Fig. 3c).
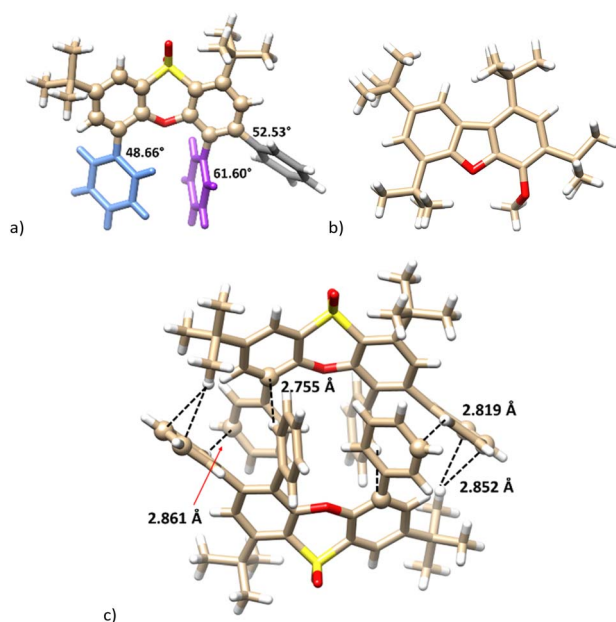

Fig. 3 Single crystal X-ray structure of compound **12**. (a) Interplanar angles of the corresponding phenyl substituents (towards phenoxathiin benzene rings shown as balls); (b) the structure of compound **11**; (c) the dimer of **12** with selected π–π and CH–π interactions.

A reaction with *tert*-butyllithium gave the product **11** containing two Bu^t groups. The ^{1}H NMR spectrum (CDCl$_3$, 400 MHz) demonstrated two doublets in the aromatic region (8.12 and 7.40 ppm, J = 1.9 Hz) and one singlet at 7.22 ppm, as expected for compounds formed by the cleavage of the SO$_2$ bridges in the macrocycle **9**. However, the HRMS ESI$^+$ surprisingly showed peaks at *m/z* 423.3261 [M + H]$^+$ and 445.3075 [M + Na]$^+$ (calc. 423.3257 [**11** + H]$^+$ and 445.3077 [**11** + Na]$^+$) corresponding to the formation of a dibenzofuran skeleton. This assumption was confirmed by a single-crystal X-ray analysis, which proved the extrusion of a SO$_2$ fragment within the heterocyclic moiety (for X-ray structure see Fig. 3b).

The formation of the planar dibenzofuran derivative **11** is surprising because the extrusion of the sulfone group to form a single bond is not a common reaction.[19] Although examples of the use of diarylsulfones for the formation of the biphenyl skeleton are known in the literature, this chemistry is based on transition metal catalysis.[20] While a similar reaction has been reported for diaryl sulfoxides,[21] to the best of our knowledge, there is no similar precedent in the literature describing the formation of a biphenyl fragment by the action of an organometallic reagent on a diaryl sulfone.

All the products mentioned indicate a markedly different reactivity/regioselectivity of the phenoxathiin macrocycle towards *C*-nucleophiles compared to previously studied *O*- or *S*-nucleophiles. As shown in Scheme 5, the *O*- and *S*-nucleophiles primarily attack the phenoxathiin backbone while the *C*-analogues cleave the SO$_2$ bridges.

The only exception in the regioselectivity of the *C*-nucleophile attack is represented by compound **13**, which was isolated as a byproduct of the butyllithium reaction (Scheme 3). The Meisenheimer-type intermediate is formed in the most activated CH position of the phenoxathiin moiety (two electron-withdrawing SO$_2$ bridges in the *ortho*- and *para*-positions) and finally quenched during the acidic workup. As a result, the corresponding macrocycle **13** bearing the cyclohexadiene ring, was obtained in a 4% yield.

According to the X-ray analysis, compound **13** crystallized in a monoclinic system, a space group $P2_1/c$ and adopted the *partial cone* conformation. As expected, the *n*-butyl group was added from the outside the cavity and is oriented *cis*- with the neighbour CH bond of the cyclohexadiene system (see Fig. 4a and b).

The unanticipated behavior of sulfone **9** towards organolithium reagents prompted us to also test monosulfoxide **9′** in similar reactions (Scheme 6). The reaction of **9′** with 2 equiv. of *n*-BuLi was carried out at the standard conditions used for compound **9** (60 °C, 1 h). It is worth noting that no substitution
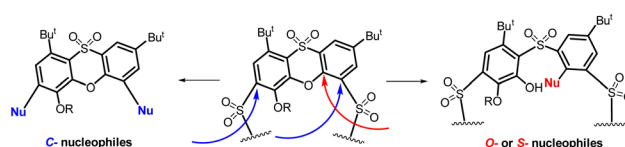
Scheme 5 Nucleophilic aromatic substitution of the phenoxathiin-based thiacalixarene **9** – primary attack of the nucleophile.
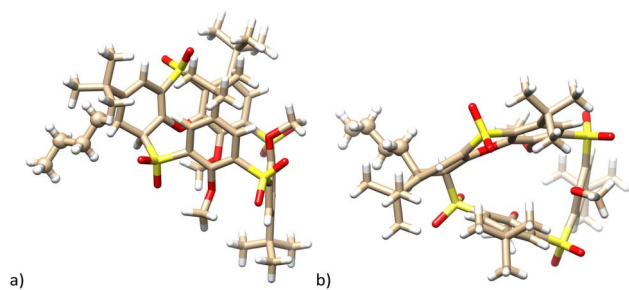
Paper

Fig. 4 Single crystal X-ray structure of the compound **13**. (a) Side view; (b) top view; butyl group is shown as balls for better clarity.

of SO$_2$ bridges was observed. Instead, the reaction occurred at the sulfoxide group, leading to the isolation of the two products, **14** and **15**, in low yields.

There were 9 signals in the aromatic part of the ^{1}H NMR spectrum of compound **15**: seven doublets possessing *meta*-coupling constants ($J \approx 2.5$ Hz) and two signals corresponding to direct *ortho*-coupling ($J \approx 8.5$ Hz). In our previous study, we reported that thiacalix[4]arenes bearing one oxidized bridge (monosulfoxide) can react with organolithium compounds (BuLi) to form cleaved linear tetramers.[22] Technically speaking, the sulfoxide group is cleaved in the form of dibutyl sulfoxide,[21b] while the remaining dianion is protonated during the work-up of the reaction mixture.

The formation of compound **15** is exactly the same type of reaction. As illustrated in Scheme 7 (upper part), the addition of BuLi leads to the hypervalent sulfurane species **A** (considered as a transition state) which provides a monoanion **B** (ligand exchange reaction) stabilized by the presence of the SO$_2$ group in the *para* position. The second attack of BuLi gives rise to another sulfurane-based species **C**, which, after removal of proton from the alpha position of dibutyl sulfoxide and cleavage of the corresponding sulfoxide enolate (synchronously or sequentially), forms an aromatic anion **D**. The final protonation of this intermediate then generates compound **15**.

The X-ray analysis corroborated the structure of compound **15**, which crystalized in a triclinic system, a space group $P\bar{1}$ (Fig. 5). Removing the sulfoxide from the molecule changes the conformation, which can be assigned as the *1,3-alternate*. Due to the *ortho*-bridge (–O–), the cavity is significantly distorted, deviating from the original square shape of thiacalix[4]arenes (Fig. 5a and b). In addition to many other interactions (not shown), the SO$_2$···HC(ar) interactions are essential for the crystal packing of **15**. Fig. 5c shows the formation of a dimeric motif consisting of both enantiomers, held together by four
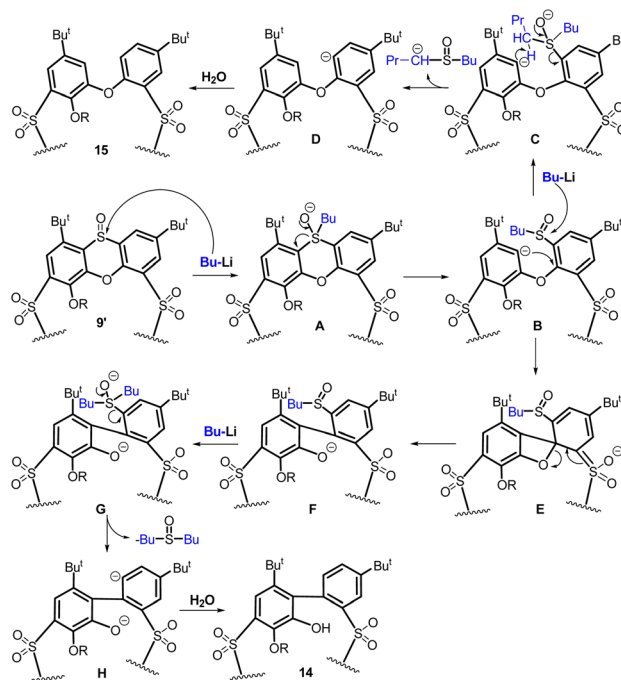
Scheme 7 Aromatic nucleophilic substitution of compound **9'**: proposed mechanisms of phenoxathiine cleavage (compound **15**) and the biphenyl fragment formation (compound **14**).

hydrogen bond interactions between the S=O and H–C(ar) (S=O···HC distances = 2.450 and 2.717 Å).

Since compound **15** represents a completely new type of macrocyclic skeleton, we investigated its behavior in solution. As indicated by low-temperature ^{1}H NMR spectra (500 MHz,
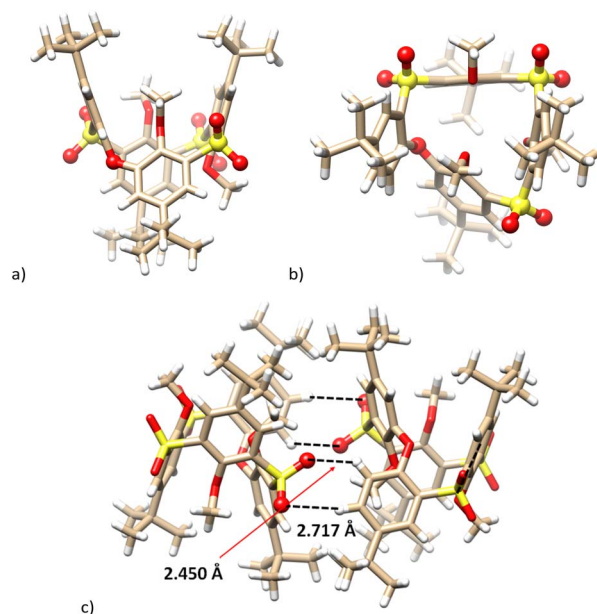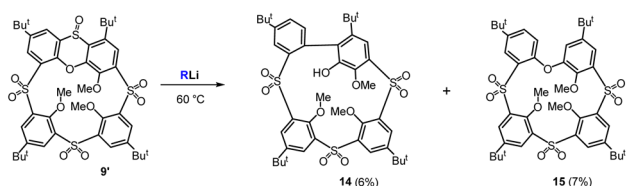

Fig. 5 Single crystal X-ray structure of the compound **15**. (a) Side view; (b) top view; bridging moieties shown as balls for better clarity; (c) dimeric motif in the crystal packing showing the S=O···H–C(ar) intermolecular HB interactions (interacting atoms shown as balls).

Scheme 6 Cleavage of compound **9'** by organolithium compounds.

CD$_2$Cl$_2$), the number of signals and their splitting pattern did not change from rt (298 K) down to 173 K, indicating that the compound existed in the form of a single conformer (atropisomer) throughout the whole temperature range (see Fig. S28 and S29‡). Similarly, heating a solution of compound **15** in CDCl$_2$–CDCl$_2$ showed no visible changes (see Fig. S30 and S31‡) in the ^{1}H NMR spectrum up to the highest achievable temperature (403 K). Macrocycle **15** is thus conformationally stable over the entire temperature range. It is therefore obvious that the introduction of a direct *ortho*-connection between the aromatic subunits leads to the immobilization of macrocyclic skeleton even with the smallest possible substituents (methyls) on the lower rim.

The molecular mass in the HRMS (ESI$^+$) spectrum of compound **14** (m/z = 849.2766) matched the predicted value for a molecule with a cleaved SO$_2$ group (m/z calc. = 849.2771 [M + Na]$^+$ for C$_{43}$H$_{54}$O$_{10}$S$_3$Na). This result was astonishing since we had not observed this reactivity before. Based on the splitting and the multiplicity of signals in the ^{1}H NMR spectrum (5 × doublet with *meta* coupling, 2 × *ortho* coupling, 1 singlet in the aromatic part), we assumed that the macrocyclic nature of the product was preserved.

Since it was impossible to assign the structure based on the spectroscopic examination alone, it was unambiguously confirmed using the single crystal X-ray structural analysis. Compound **14** crystalized in a monoclinic system, a space group $P2_1/c$ (Fig. 6), and its structure can be described as the *partial cone* conformation. The resulting cavity is profoundly distorted since the molecule contains a direct bond between two aromatic subunits. The presence of the biphenyl fragment (blue color in Fig. 6) makes the whole system extremely rigid. The effort to minimize the internal tension causes a significant rotation of the corresponding phenyl rings, with interplanar angle being

76.39°. To the best of our knowledge, compound **14** is the first example of a calixarene-like system based on a biphenyl fragment.

A possible mechanism for the formation of compound **14** is shown in Scheme 7, bottom part. The key step is apparently the intramolecular attack of the aromatic anion **B** to form the biphenyl fragment **F** (probably *via* the transition state **E**). The subsequent removal of the sulfoxide group is then just an application of the aforementioned chemistry (**F** → **G** → **H** → **14**).

The formation of derivatives **14** and **15** demonstrates an unprecedented reactivity of the phenoxathiin macrocycles, which allow, depending on the nucleophile used, considerable changes in the cavity shape while maintaining the macrocyclic skeleton. The use of *O*-nucleophiles leads to the formation of a system possessing bridges in the *meta*- and *para*- (*m-,m-,m-,p-*) positions, while the use of organolithium reagents gives very rigid macrocyclic systems with the *m-,m-,o-,p-* (**14**) and *m-,m-,m-,o-* (**15**) bridge arrangements. The examples nicely demonstrate the dramatic differences in the chemical transformations available in the calixarene and thiacalixarene series. Further development of thiacalixarene chemistry can result in hitherto unknown macrocyclic systems potentially useful in supramolecular chemistry.

Conclusions

In conclusion, the reactivity of fully and partially oxidized forms of phenoxathiin-based thiacalix[4]arene **9** and **9′** towards organolithium reagents was studied. The presence of electron-withdrawing groups (SO$_2$, SO) and the considerable internal strain caused by the condensed heterocyclic moiety render these molecules susceptible to nucleophilic attack. The reaction with various organolithium reagents provides a number of different products resulting from the cleavage of either the calixarene skeleton or the phenoxathiin group or both ways simultaneously. This enables the preparation of thiacalixarene analogues with unusual structural features, including systems containing a biphenyl fragment as a part of the macrocyclic skeleton.

Due to their complexity, the above-described transformations of phenoxathiin-based thiacalix[4]arenes probably will not find general application in supramolecular chemistry. On the other hand, the mentioned reactions have no analogues in the chemistry of classical calixarenes, thus clearly demonstrating the fundamental differences between the two systems (calixarenes *vs.* thiacalixarenes). At the same time, however, they indicate the surprising synthetic potential and unusual derivatization possibilities of this interesting subgroup of thiacalixarenes.

Fig. 6 Single crystal X-ray structure of compound **14**. (a) Side view; (b) top view, biphenyl fragments shown as blue balls.

Experimental

General experimental procedures

All the commercially obtained chemicals were used as received, without further purification. The solvents were dried and distilled using conventional methods. For the melting point
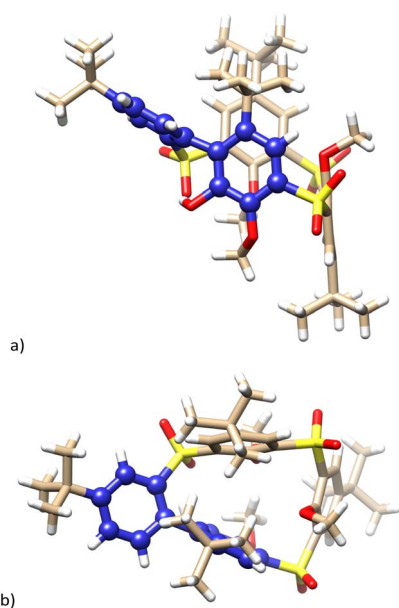
studies, Heiztisch Mikroskop–Polytherm A (Wagner & Munz, München, Germany) was used. The ^{1}H, ^{13}C{^{1}H} NMR spectra were recorded on an Agilent 400-MR DDR2 and JEOL-ECZL400G ([1]H: 400 MHz, [13]C: 100 MHz). The chemical shifts (δ) are reported in parts per million (ppm) and were referenced to the residual peaks of the solvent or TMS as an internal standard; the coupling constants (J) are expressed in Hz. All the NMR data were processed and displayed using MestReNova software. The electrospray ionization mass spectra (ESI-MS) were recorded using an LTQ Orbitrap Velos-hybrid ion-trap-Orbitrap (Thermo Scientific, Waltham, MA, USA). The purity of the substances and courses of the reactions were monitored using thin layer chromatography (TLC), using silica gel 60 F254 on aluminium-backed sheets (Merck) and analysed at 254 nm. The column chromatography was conducted on silica gel 60 with particle sizes of 0.063–0.200 mm (Merck).

Synthetic procedures

Spirocompound 2. Thiacalixarene **II** (5.00 g, 6.94 mmol) was dissolved in 450 mL of CHCl$_3$ and 150 mL of MeOH and the mixture was cooled to 0 °C. Chloramine T trihydrate (2.96 g, 10.59 mmol) was added and the reaction mixture was stirred at 0 °C for 1.5 h. The organic phase was then evaporated to dryness. 250 mL of water and 150 mL of sodium chloride solution were poured into the flask. The crude product was extracted with DCM (3 × 50 mL). The organic phase was then dried over MgSO$_4$ and evaporated to dryness. The crude product was dispersed in 150 mL of MeOH and the product was filtered off. Thiacalixarene **2** was obtained in 61% (3.02 g) yield as an orange powder. ^{1}H NMR (CDCl$_3$, 400 MHz, 298 K) δ (ppm): δ 8.26 (s, 1H, Ar-OH), 7.80 (s, 1H, Ar-OH), 7.64–7.62 (m, 1H, Ar-H), 7.54 (d, J = 2.5 Hz, 1H, Ar-H), 7.53 (d, J = 2.2 Hz, 1H, Ar-H), 7.44 (d, J = 2.4 Hz, 1H, Ar-H), 7.33 (d, J = 2.0 Hz, 1H, Ar-H), 7.27 (d, J = 2.4 Hz, 1H, Ar-H), 7.04 (d, J = 2.0 Hz, 1H, Ar-H), 6.44 (d, J = 2.3 Hz, 1H, Ar-H), 1.25 (s, 9H, t-Bu), 1.24 (s, 9H, t-Bu), 1.24 (s, 9H, t-Bu), 1.22 (s, 9H, t-Bu). All data are consistent with the literature.[9,11a]

Thiacalixarene 4. Thiacalixarene **2** (3.00 g, 4.17 mmol) was suspended in 600 mL of acetonitrile. 45 mL of 36% HCl was added and the reaction mixture was stirred for 45 min under reflux. The organic phase was then evaporated to dryness. The crude product was triturated by chloroform (4 × 40 mL). The crude product was then dispersed in chloroform and the mixture was filtered off. Filtrate was evaporated to dryness and the crude product was recrystallized from chloroform/acetonitrile mixture. Thiacalixarene **4** was obtained in 80% (2.41 g) yield as white crystals. ^{1}H NMR (CDCl$_3$, 400 MHz, 298 K) δ (ppm): 8.40 (s, 1H, Ar-OH), 8.39 (s, 1H, Ar-OH), 7.84 (s, 1H, Ar-OH), 7.78 (d, J = 2.3 Hz, 1H, Ar-H), 7.49 (d, J = 2.4 Hz, 1H, Ar-H), 7.45 (d, J = 2.4 Hz, 1H, Ar-H), 7.38 (d, J = 2.4 Hz, 1H, Ar-H), 7.37 (d, J = 2.4 Hz, 1H, Ar-H), 7.34 (s, 1H, Ar-H), 7.27 (d, J = 2.3 Hz, 1H, Ar-H), 1.43 (s, 9H, t-Bu), 1.31 (s, 9H, t-Bu), 1.16 (s, 9H, t-Bu), 1.14 (s, 9H, t-Bu). All data are consistent with the literature.[11a]

Thiacalixarene 9. Thiacalixarene **4** (3.20 g, 4.45 mmol) was dissolved in 45 mL of chloroform. 15 mL of trifluoroacetic acid and 42 mL of 30% hydrogen peroxide were added and the

reaction mixture was stirred and heated at 62 °C for 4 days. The crude product was extracted with chloroform (3 × 80 mL). Organic layer was washed with water, dried over MgSO$_4$ and evaporated to yield the crude intermediate **8** (3.75 g, 98%, white solid). This compound was dissolved in 350 mL of dry acetone, Cs$_2$CO$_3$ (30 g, 92.08 mmol) and MeI (5 mL, 80.32 mmol) were added and the reaction mixture was stirred and heated at 52 °C for 2 days. The organic phase was then evaporated to dryness. Water 90 mL was added and the crude product was extracted with chloroform (3 × 80 mL). Organic layer was washed with 1 M HCl and water, dried over MgSO$_4$ and separated by column chromatography on silica gel (eluent = cyclohexane : EtOAc = 4 : 1, v/v). Compound **9** was obtained as a white powder (2.79 g) in 70% yield (from **4**). ^{1}H NMR (CDCl$_3$, 400 MHz, 298 K) δ (ppm): 8.56 (d, J = 2.4 Hz, 1H, Ar-H), 8.48 (d, J = 2.5 Hz, 1H, Ar-H), 8.38 (d, J = 2.5 Hz, 1H, Ar-H), 8.37 (d, J = 2.3 Hz, 1H, Ar-H), 8.09 (d, J = 2.5 Hz, 1H, Ar-H), 8.01 (s, 1H, Ar-H), 6.44 (d, J = 2.5 Hz, 1H, Ar-H), 4.14 (s, 3H, –O–CH$_3$), 3.80 (s, 3H, –O–CH$_3$), 3.43 (s, 3H, –O–CH$_3$), 1.60 (s, 9H, t-Bu), 1.50 (s, 9H, t-Bu), 1.49 (s, 9H, t-Bu), 0.81 (s, 9H, t-Bu). All data are consistent with the literature.[12]

Thiacalixarene 9′. Thiacalixarene **4** (3.20 g, 4.45 mmol) was dissolved in 62 mL of CHCl$_3$. Then 21 mL of trifluoroacetic acid and 62 mL of 30% hydrogen peroxide were added and the reaction mixture was stirred at rt in the dark overnight. The crude product was extracted with DCM. The organic phase was then dried over MgSO$_4$ and evaporated to dryness to yield the crude intermediate **8′** (2.90 g, 78%). This compound was dissolved in 275 mL of dry acetone. Cs$_2$CO$_3$ (24.5 g, 75.19 mmol) and MeI (4 mL, 64.25 mmol) were added and the reaction mixture was stirred and heated at 52 °C for 1 day. The organic phase was then evaporated to dryness. Water (80 mL) was added and the crude product was extracted with chloroform (3 × 70 mL). Organic layer was washed with 1 M HCl and water, dried over MgSO$_4$ and separated by column chromatography on silica gel (eluent = cyclohexane : EtOAc = 2.5 : 1, v/v). Compound **9′** (3.00 g) was obtained in 76% yield (from **4**) as a white powder. ^{1}H NMR (CDCl$_3$, 400 MHz, 298 K) δ (ppm): 8.58 (d, J = 2.3 Hz, 1H, Ar-H), 8.46 (d, J = 2.5 Hz, 1H, Ar-H), 8.39 (d, J = 2.5 Hz, 1H, Ar-H), 8.20 (d, J = 2.3 Hz, 1H, Ar-H), 8.04 (d, J = 2.5 Hz, 1H, Ar-H), 7.87 (s, 1H, Ar-H), 6.39 (d, J = 2.5 Hz, 1H, Ar-H), 4.15 (s, 3H, –O–CH$_3$), 3.78 (s, 3H, –O–CH$_3$), 3.55 (s, 3H, –O–CH$_3$), 1.59 (s, 9H, t-Bu), 1.50 (s, 9H, t-Bu), 1.50 (s, 9H, t-Bu), 0.73 (s, 9H, t-Bu). All data are consistent with the literature.[12]

Compound 10a. Thiacalixarene **9** (0.30 g, 0.34 mmol) was dissolved in 32 mL of dry THF. 1.6 M MeLi in Et$_2$O (1.3 mL, 2 mmol) was added and the reaction mixture was stirred and heated at 60 °C for 1 h under argon atmosphere. Methanol (10 mL) was added and the organic phase was evaporated to dryness. Water (30 mL) was added and the crude product was extracted with chloroform (3 × 30 mL), the organic phase was then washed with 1 M HCl and with water, dried over MgSO$_4$ and separated by column chromatography on silica gel (eluent = cyclohexane : DCM = 1 : 3, v/v). Compound **10a** was obtained in 12% (15.8 mg) yield as white film. ^{1}H NMR (CDCl$_3$, 400 MHz, 298 K) δ (ppm): 7.87 (d, J = 2.4 Hz, 1H, Ar-H), 7.50 (d, J = 2.4 Hz, 1H, Ar-H), 7.24 (s, 1H, Ar-H), 3.98 (s, 3H, –O–CH$_3$), 2.56 (s, 3H, –CH$_3$), 2.36 (s, 3H, –CH$_3$), 1.65 (s, 9H, t-Bu), 1.35 (s, 9H, t-Bu). [13]C

NMR (100 MHz, CDCl$_3$, 298 K) δ (ppm): 151.65, 150.08, 149.12, 147.65, 146.34, 144.23, 135.87, 135.74, 132.85, 127.35, 126.17, 126.12, 125.66, 117.54, 60.99, 37.14, 34.99, 34.35, 32.24, 31.41, 30.44, 16.54, 15.77. HRMS (ESI$^+$) (C$_{23}$H$_{30}$O$_4$S) m/z calc.: 425.1757 [M + Na]$^+$, found: 425.1759 [M + Na]$^+$.

Compound 10b. Thiacalixarene **9** (0.30 g, 0.34 mmol) was dissolved in 32 mL of dry THF. 0.5 M EtLi in benzene : cyclohexane (4 mL, 2 mmol) was added and the reaction mixture was stirred and heated at 60 °C for 1 h under argon atmosphere. Methanol (10 mL) was added and the organic phase was evaporated to dryness. Water (30 mL) was added and the crude product was extracted with chloroform (3 × 30 mL), the organic phase was then washed with 1 M HCl and with water, dried over MgSO$_4$ and separated by column chromatography on silica gel (eluent = cyclohexane : DCM = 1 : 1, v/v). Compound **10b** was obtained in 70% (101.2 mg) yield as white solid. Mp = 139–142 °C. ^{1}H NMR (DMSO-d_6, 400 MHz, 298 K) δ (ppm): 7.81 (d, J = 2.4 Hz, 1H, Ar-H), 7.78 (d, J = 2.3 Hz, 1H, Ar-H), 7.40 (s, 1H, Ar-H), 3.99 (s, 3H, –O–CH$_3$), 3.05–2.95 (m, 2H, –CH$_2$–), 2.80–2.70 (m, 2H, –CH$_2$–), 1.61 (s, 9H, t-Bu), 1.37 (s, 9H, t-Bu), 1.36–1.33 (m, 3H, –CH$_3$), 1.26–1.21 (m, 3H, –CH$_3$). ^{13}C NMR (DMSO-d_6, 100 MHz, 298 K) δ (ppm): 149.73, 148.66, 148.26, 146.17, 143.84, 142.18, 133.84, 132.53, 126.29, 126.14, 124.87, 116.82, 61.99, 37.28, 35.19, 32.25, 31.39, 23.41, 22.98, 15.18, 14.92. HRMS (ESI$^+$) (C$_{25}$H$_{34}$O$_4$S) m/z calc.: 431.2250 [M + H]$^+$, found: 431.2250 [M + H]$^+$.

Compounds 10c and 13. Thiacalixarene **9** (0.30 g, 0.34 mmol) was dissolved in 32 mL of dry THF. 2.5 M n-BuLi in hexane (0.48 mL, 1.2 mmol) was added and the reaction mixture was stirred and heated at 60 °C for 1 h under argon atmosphere. Methanol (10 mL) was added and the organic phase was evaporated to dryness. Water (30 mL) was added and the crude product was extracted with chloroform (3 × 30 mL), the organic phase was then washed with 1 M HCl and with water, dried over MgSO$_4$ and separated by column chromatography on silica gel (eluent = cyclohexane : DCM = 1 : 1, v/v). Compound **10c** was obtained in 38% (63 mg) yield as a white solid together with 4% (12.4 mg) yield of compound **13** as a white solid.

Data for 10c. Mp = 87–89 °C. ^{1}H NMR (400 MHz, CDCl$_3$, 298 K) δ (ppm): 7.87 (d, J = 2.4 Hz, 1H, Ar-H), 7.47 (d, J = 2.4 Hz, 1H, Ar-H), 7.23 (s, 1H, Ar-H), 3.98 (s, 3H, –O–CH$_3$), 2.96–2.90 (m, 2H, –CH$_2$–), 2.71–2.66 (m, 2H, –CH$_2$–), 1.75–1.69 (m, 2H, –CH$_2$–), 1.65 (s, 9H, t-Bu), 1.61–1.56 (m, 2H, –CH$_2$–), 1.50–1.45 (m, 2H, –CH$_2$–), 1.42–1.36 (m, 2H, –CH$_2$–), 1.35 (s, 9H, t-Bu), 1.01–0.97 (m, 3H, –CH$_3$), 0.97–0.93 (m, 3H, –CH$_3$). ^{13}C NMR (100 MHz, CDCl$_3$, 298 K) δ (ppm): 150.21, 149.06, 147.68, 146.22, 144.26, 140.34, 132.15, 132.08, 126.39, 126.24, 124.82, 117.67, 61.62, 37.21, 35.03, 32.83, 32.48, 32.28, 31.44, 30.46, 30.24, 30.09, 22.93, 22.81, 14.10, 14.05. HRMS (ESI$^+$) (C$_{29}$H$_{42}$O$_4$S) m/z calc.: 509.2696 [M + Na]$^+$, found: 509.2695 [M + Na]$^+$.

Data for 13. Mp = 195–197 °C. ^{1}H NMR (400 MHz, CDCl$_3$, 298 K) δ (ppm): 8.41 (d, J = 2.5 Hz, 1H, Ar-H), 8.39 (d, J = 2.5 Hz, 1H, Ar-H), 8.27 (s, 1H, Ar-H), 8.20 (d, J = 2.5 Hz, 1H, Ar-H), 8.09 (s, 1H, Ar-H), 7.42 (d, J = 2.6 Hz, 1H, Ar-H), 6.36 (s, 1H, Ar-H), 4.36 (d, J = 1.1 Hz, 1H, Ar-H), 3.98 (s, 3H, –O–CH$_3$), 3.76 (s, 3H, –O–CH$_3$), 3.55 (s, 3H, –O–CH$_3$), 1.83–1.73 (m, 2H, –CH$_2$–), 1.59 (s, 9H, t-Bu), 1.48 (s, 9H, t-Bu), 1.40–1.36 (m, 2H, –CH$_2$–) 1.32 (s,

9H, t-Bu), 1.27–1.24 (m, 2H, –CH$_2$–) 1.21 (s, 9H, t-Bu), 0.93–0.87 (m, 3H, –CH$_3$). ^{13}C NMR (100 MHz, CDCl$_3$, 298 K) δ (ppm): 155.71, 154.09, 153.24, 148.63, 146.96, 146.77, 145.63, 144.68, 144.34, 142.33, 137.97, 137.64, 137.44, 136.25, 135.86, 134.69, 132.93, 132.51, 132.14, 130.62, 130.30, 123.32, 118.93, 105.59, 73.48, 67.45, 66.62, 65.80, 62.43, 38.52, 38.09, 37.07, 35.46, 35.20, 35.13, 32.36, 31.31, 31.10, 30.99, 30.27, 28.30, 22.39, 14.08. HRMS (ESI$^+$) (C$_{47}$H$_{62}$O$_{12}$S$_4$) m/z calc.: 969.3016 [M + Na]$^+$, found: 969.3008 [M + Na]$^+$.

Compound 11. Thiacalixarene **9** (0.30 g, 0.34 mmol) was dissolved in 32 mL of dry THF. 1.7 M t-BuLi in pentane (1.2 mL, 2.04 mmol) was added and the reaction mixture was stirred and heated at 60 °C for 1 h under argon atmosphere. Methanol (10 mL) was added and the organic phase was evaporated to dryness. Water (30 mL) was added and the crude product was extracted with chloroform (3 × 30 mL), the organic phase was then washed with 1 M HCl and with water, dried over MgSO$_4$ and separated by column chromatography on silica gel (eluent = cyclohexane : DCM = 4 : 1, v/v). Compound **11** was obtained (23.0 mg) in 16% yield as white solid. Mp = 163–165 °C. ^{1}H NMR (400 MHz, CDCl$_3$, 298 K) δ (ppm): 8.13 (d, J = 1.9 Hz, 1H, Ar-H), 7.41 (d, J = 2.0 Hz, 1H, Ar-H), 7.23 (s, 1H, Ar-H), 4.20 (s, 3H, –O–CH$_3$), 1.63 (s, 9H, t-Bu), 1.60 (s, 9H, t-Bu), 1.48 (s, 9H, t-Bu), 1.44 (s, 9H, t-Bu). ^{13}C NMR (100 MHz, CDCl$_3$, 298 K) δ (ppm): 152.54, 144.42, 139.63, 138.78, 133.57, 123.67, 120.71, 120.56, 117.71, 60.67, 35.69, 35.46, 35.27, 34.78, 32.14, 30.83, 30.24, 30.17. HRMS (ESI$^+$) (C$_{29}$H$_{42}$O$_2$) m/z calc.: 445.3077 [M + Na]$^+$, found: 445.3075 [M + Na]$^+$.

Compound 12. Thiacalixarene **9** (0.30 g, 0.34 mmol) was dissolved in 32 mL of dry THF. 1.8 M PhLi in dibutyl ether (1 mL, 1.8 mmol) was added and the reaction mixture was stirred and heated at 60 °C for 1 h under argon atmosphere. Methanol (10 mL) was added and the organic phase was evaporated to dryness. Water (30 mL) was added and the crude product was extracted with chloroform (3 × 30 mL), the organic phase was then washed with 1 M HCl and with water, dried over MgSO$_4$ and separated by column chromatography on silica gel (eluent = cyclohexane : DCM = 2 : 1, v/v). Compound **12** was obtained in 10% (18.5 mg) yield as white solid. Mp = 241–243 °C. ^{1}H NMR (400 MHz, CDCl$_3$, 298 K) δ (ppm): 8.08 (d, J = 2.5 Hz, 1H, Ar-H), 7.55 (d, J = 2.4 Hz, 1H, Ar-H), 7.50 (s, 1H, Ar-H), 7.17–7.08 (m, 6H, Ar-H), 7.05–6.99 (m, 2H, Ar-H), 6.96–6.90 (m, 3H, Ar-H), 6.82–6.74 (m, 4H, Ar-H), 1.76 (s, 9H, t-Bu), 1.38 (s, 9H, t-Bu). ^{13}C NMR (100 MHz, CDCl$_3$, 298 K) δ (ppm): 154.32, 148.84, 148.30, 147.92, 146.06, 140.20, 135.92, 134.68, 133.40, 131.78, 131.15, 130.47, 129.52, 128.96, 128.31, 127.88, 127.50, 127.46, 127.33, 127.25, 126.62, 126.60, 126.01, 119.29, 37.72, 35.16, 32.34, 31.42, 29.85. HRMS (ESI$^+$) (C$_{38}$H$_{36}$O$_3$S) m/z calc.: 595.2277 [M + Na]$^+$, found: 595.2280 [M + Na]$^+$.

Compounds 14 and 15. Thiacalixarene **9′** (0.3 g, 0.34 mmol) was dissolved in 32 mL of dry THF. 2.5 M n-BuLi in hexane (0.28 mL, 0.7 mmol) was added and the reaction mixture was stirred and heated at 60 °C for 1 h under argon atmosphere. Methanol (10 mL) was added and the organic phase was evaporated to dryness. Water (30 mL) was added and the crude product was extracted with chloroform (3 × 30 mL), the organic phase was then washed with 1 M HCl and with water, dried over MgSO$_4$

and separated by column chromatography on silica gel (eluent = cyclohexane : EtOAc = 4 : 1, v/v). Compound **14** was obtained in 6% (16.7 mg) yield together with 7% (19 mg) yield of compound **15** (both compounds as a white solid).

*Data for **14**.* Mp > 350 °C. ^{1}H NMR (400 MHz, CDCl$_3$, 298 K) δ (ppm): 8.49 (d, $J = 2.0$ Hz, 1H, Ar-H), 8.44 (d, $J = 2.4$ Hz, 1H, Ar-H), 8.33 (d, $J = 2.5$ Hz, 1H, Ar-H), 8.30 (d, $J = 2.5$ Hz, 1H, Ar-H), 7.73–7.69 (m, 2H, Ar-H), 7.61 (d, $J = 2.5$ Hz, 1H, Ar-H), 7.28 (d, $J = 8.0$ Hz, 1H, Ar-H), 6.14 (s, 1H, –OH), 3.89 (s, 3H, –O–CH$_3$), 3.65 (s, 3H, –O–CH$_3$), 3.60 (s, 3H, –O–CH$_3$), 1.46 (s, 9H, *t*-Bu), 1.45 (s, 9H, *t*-Bu), 1.31 (s, 9H, *t*-Bu), 0.72 (s, 9H, *t*-Bu). ^{13}C NMR (100 MHz, CDCl$_3$, 298 K) δ (ppm): 154.20, 153.97, 153.92, 148.06, 147.98, 146.78, 146.00, 141.59, 140.57, 140.35, 136.68, 136.55, 134.33, 134.23, 133.41, 133.22, 132.75, 132.73, 132.21, 131.22, 130.87, 130.70, 125.75, 125.34, 66.22, 66.13, 60.98, 36.96, 35.53, 35.46, 35.36, 33.00, 31.35, 30.97, 29.56. HRMS (ESI$^+$) (C$_{43}$H$_{54}$O$_{10}$S$_3$) *m/z* calc.: 849.2771 [M + Na]$^+$, found: 849.2766 [M + Na]$^+$.

*Data for **15**.* Mp > 350 °C. ^{1}H NMR (400 MHz, CDCl$_3$, 298 K) δ (ppm): 8.37 (d, $J = 2.5$ Hz, 1H, Ar-H), 8.34 (d, $J = 2.5$ Hz, 1H, Ar-H), 8.26 (d, $J = 2.5$ Hz, 1H, Ar-H), 8.13 (d, $J = 2.5$ Hz, 1H, Ar-H), 7.74 (d, $J = 2.3$ Hz, 1H, Ar-H), 7.72 (d, $J = 2.5$ Hz, 1H, Ar-H), 7.61 (dd, $J = 8.7, 2.5$ Hz, 1H, Ar-H), 7.09 (d, $J = 2.3$ Hz, 1H, Ar-H), 7.07 (d, $J = 4.1$ Hz, 1H, Ar-H), 4.07 (s, 3H, –O–CH$_3$), 3.68 (s, 3H, –O–CH$_3$), 3.03 (s, 3H, –O–CH$_3$), 1.44 (s, 9H, *t*-Bu), 1.39 (s, 9H, –O–CH$_3$), 1.23 (s, 9H, –O–CH$_3$), 1.14 (s, 9H, –O–CH$_3$). ^{13}C NMR (100 MHz, CDCl$_3$, 298 K) δ (ppm): 154.94, 153.63, 150.01, 147.88, 147.80, 147.14, 146.44, 146.07, 144.33, 137.33, 136.96, 135.94, 135.88, 135.79, 132.85, 132.26, 132.09, 132.02, 131.94, 131.82, 126.04, 120.41, 118.94, 117.25, 66.71, 65.26, 61.19, 35.35, 35.11, 34.97, 34.81, 31.41, 31.27, 31.26, 31.04. HRMS (ESI$^+$) (C$_{43}$H$_{54}$O$_{10}$S$_3$) *m/z* calc.: 849.2771 [M + Na]$^+$, found: 849.2769 [M + Na]$^+$.

Theoretical calculations

The calculation was performed using GFN2-XTB method,[17] with the transition state optimization and vibrational frequency calculation performed by ORCA.[23] The GFN2-XTB calculations used ALPB formalism[24] for implicit solvent with parameters for THF. The nature of transition state was confirmed by presence of one imaginary vibrational mode along the expected reaction coordinate.

X-ray measurements

Crystallographic data for 10b. $M = 430.48$ g mol^{-1}, monoclinic system, space group $P2_1/n$, $a = 10.1548(4)$ Å, $b = 13.1857(5)$ Å, $c = 17.8205(7)$ Å, $\beta = 99.4068(13)°$, $Z = 4$, $V = 2354.05(16)$ Å^3, $D_c = 1.215$ g cm^{-3}, $\mu_{CuK\alpha} = 1.437$ mm^{-1}, crystal dimensions of $0.50 \times 0.39 \times 0.14$ mm. Data were collected at 180(2) K on a Bruker D8 VENTURE system[25] equipped with charge-integrating pixel array detector Photon II 7, a multilayer monochromator and a CuKα Incoatec microfocus sealed tube ($\lambda = 1.54180$ Å) using combined φ and ω scans at 180 K. The structure was solved by charge flipping methods[26] and anisotropically refined by full matrix least squares on F^2 using the CRYSTALS[27] to final value of $R = 0.0369$ and w$R = 0.1038$ using 4482 independent reflections ($\theta_{max} = 72.2°$), 300 parameters and 0 restrains. The hydrogen atoms bonded to carbon atoms were placed in calculated positions refined with a riding constrains. MCE[28] was used for visualization of electron density maps. The occupancy of disordered functional group was constrained to full. The structure was deposited into Cambridge Structural Database under number CCDC 2335766.‡

Crystallographic data for 10c. $M = 486.72$ g mol^{-1}, monoclinic system, space group $P2_1/c$, $a = 10.46238(7)$ Å, $b = 26.51526(17)$ Å, $c = 9.96612(8)$ Å, $\beta = 101.3066(7)°$, $Z = 4$, $V = 2711.07(3)$ Å^3, $D_c = 1.192$ g cm^{-3}, $\mu(CuK\alpha) = 1.30$ mm^{-1}, crystal dimensions of $0.42 \times 0.06 \times 0.04$ mm. Data were collected at 95(2) K on a Rigaku OD Supernova equipped with Atlas S2 CCD detector using microfocus sealed X-ray tube, Cu-Kα radiation ($\lambda = 1.54184$ Å). The structure was solved by charge flipping methods[26] and anisotropically refined by full matrix least squares on F^2 using the CRYSTALS[27] to final value $R = 0.032$ and w$R = 0.087$ using 5369 independent reflections ($\theta_{max} = 73.2°$), 307 parameters and 0 restrains. The hydrogen atoms bonded to carbon atoms were placed in calculated positions refined with a riding constrains. MCE[28] was used for visualization of electron density maps. The structure was deposited into Cambridge Structural Database under number CCDC 2336469.‡

Crystallographic data for 11. $M = 422.65$ g mol^{-1}, monoclinic system, space group $P2_1/c$, $a = 5.9326(3)$ Å, $b = 16.6120(9)$ Å, $c = 26.1176(14)$ Å, $\beta = 91.059(3)°$, $Z = 4$, $V = 2573.5(2)$ Å^3, $D_c = 1.091$ g cm^{-3}, $\mu_{CuK\alpha} = 0.504$ mm^{-1}, crystal dimensions of 0.038 mm x 0.062 mm x 0.421 mm. Data were collected at 180(2) K on a Bruker D8 VENTURE system[25] equipped with charge-integrating pixel array detector Photon II 7, a multilayer monochromator and a CuKα Incoatec microfocus sealed tube ($\lambda = 1.54180$ Å) using combined φ and ω scans at 180 K. The structure was solved by direct methods[29] and anisotropically refined by full matrix least squares on F^2 using the CRYSTALS[27] to final value of $R = 0.0525$ and w$R = 0.1486$ using 4868 independent reflections ($\theta_{max} = 70.1°$), 281 parameters and 0 restrains. The hydrogen atoms bonded to carbon atoms were placed in calculated positions refined with a riding constrains. MCE[28] was used for visualization of electron density maps. The structure was deposited into Cambridge Structural Database under number CCDC 2335767.‡

Crystallographic data for 12. $M = 572.77$ g mol^{-1}, monoclinic system, space group $P2_1/c$, $a = 11.99070(12)$ Å, $b = 11.76474(11)$ Å, $c = 21.9240(3)$ Å, $\beta = 102.9341(11)°$, $Z = 4$, $V = 3014.30(6)$ Å^3, $D_c = 1.262$ g cm^{-3}, $\mu(CuK\alpha) = 1.24$ mm^{-1}, crystal dimensions of $0.50 \times 0.39 \times 0.14$ mm. Data were collected at 120(2) K on a Rigaku OD Gemini equipped with Atlas S2 CCD detector using mirror collimated sealed X-ray tube, Cu-Kα radiation ($\lambda = 1.54184$ Å). The structure was solved by charge flipping methods[26] and anisotropically refined by full matrix least squares on F^2 using the CRYSTALS[27] to final value $R = 0.033$ and w$R = 0.092$ using 5403 independent reflections ($\theta_{max} = 67.6°$), 380 parameters and 0 restrains. The hydrogen atoms bonded to carbon atoms were placed in calculated positions refined with a riding constrains. MCE[28] was used for visualization of electron density maps. The occupancy of disordered functional group was constrained to full. The

structure was deposited into Cambridge Structural Database under number CCDC 2336466.‡

Crystallographic data for 13. $M = 1032.20$ g mol^{-1}, monoclinic system, space group $P2_1/c$, $a = 21.3670(13)$ Å, $b = 9.5552(6)$ Å, $c = 25.7750(15)$ Å, $\beta = 100.165$ (3)°, $Z = 4$, $V = 5179.8$ (5) Å^3, $D_c = 1.324$ g cm^{-3}, μ(Cu-Kα) = 3.12 mm^{-1}, crystal dimensions of $0.20 \times 0.16 \times 0.16$ mm. Data were collected at 180(2) K on a Bruker D8 Venture equipped with Photon CMOS detector using a Cu-Kα Incoatec microfocus sealed tube ($\lambda = 1.54180$ Å) with a multilayer monochromator. The structure was solved by charge flipping methods[26] and anisotropically refined by full matrix least squares on F^2 using the CRYSTALS[27] to final value $R = 0.090$ and w$R = 0.264$ using 9530 independent reflections ($\theta_{max} = 68.7°$), 653 parameters and 80 restrains. The hydrogen atoms bonded to carbon atoms were placed in calculated positions refined with a riding constrains. MCE[28] was used for visualization of electron density maps. The disordered functional groups were refined with restrained geometry. The occupancy of disordered functional group was constrained to full and refined to final occupancy ratios 606(8) : 394(8) and 771(8) : 229(8). The structure was deposited into Cambridge Structural Database under number CCDC 2336468.‡

Crystallographic data for 14. $M = 827.09$ g mol^{-1}, monoclinic system, space group $P2_1/c$, $a = 15.7249(4)$ Å, $b = 14.5795(4)$ Å, $c = 18.6923(5)$ Å, $\beta = 91.5925$ (12)°, $Z = 4$, $V = 4283.8$ (2) Å^3, $D_c = 1.282$ g cm^{-3}, μ(Cu-Kα) = 2.04 mm^{-1}, crystal dimensions of $0.32 \times 0.31 \times 0.17$ mm. Data were collected at 260(2) K on a Bruker D8 Venture equipped with Photon CMOS detector using a Cu-Kα Incoatec microfocus sealed tube ($\lambda = 1.54178$ Å) with a multilayer monochromator. The structure was solved by charge flipping methods[26] and anisotropically refined by full matrix least squares on F^2 using the CRYSTALS[27] to final value $R = 0.047$ and w$R = 0.141$ using 8132 independent reflections ($\theta_{max} = 70.3°$), 622 parameters and 142 restrains. The hydrogen atoms bonded to carbon atoms were placed in calculated positions refined with a riding constrains, while hydrogen atoms bonded to oxygen were refined using soft restraints. MCE[28] was used for visualization of electron density maps. The disordered functional groups were refined with restrained geometry. The occupancy of disordered functional group was constrained to full and refined to final occupancy ratios 411(7) : 310(13) : 0.279(12) and 626(5) : 374(5). The structure was deposited into Cambridge Structural Database under number CCDC 2336470.‡

Crystallographic data for 15. $M = 827.09$ g mol^{-1}, triclinic system, space group $P\bar{1}$, $a = 11.7442(4)$ Å, $b = 14.1049(5)$ Å, $c = 15.5420(6)$ Å, $\alpha = 63.6900$ (12)°, $\beta = 70.5333$ (14)°, $\gamma = 73.0289$ (13)°, $Z = 2$, $V = 2144.02$ (14) Å^3, $D_c = 1.281$ g cm^{-3}, μ(Mo-Kα) = 0.23 mm^{-1}, crystal dimensions of $0.45 \times 0.39 \times 0.21$ mm. Data were collected at 180(2) K on a Bruker D8 Venture equipped with Photon CMOS detector using a Mo-Kα Incoatec microfocus sealed tube ($\lambda = 0.71073$ Å) with a multilayer monochromator. The structure was solved by charge flipping methods[26] and anisotropically refined by full matrix least squares on F^2 using the CRYSTALS[27] to final value $R = 0.051$ and w$R = 0.160$ using 11 495 independent reflections ($\theta_{max} = 29.1°$), 505 parameters and 0 restrains. The hydrogen atoms bonded to carbon atoms

were placed in calculated positions refined with a riding constrains. MCE[28] was used for visualization of electron density maps. The occupancy of disordered functional group was constrained to full. The structure was deposited into Cambridge Structural Database under number CCDC 2336467.‡

Conflicts of interest

There are no conflicts of interest to declare.

Acknowledgements

Notes and references

1 H. Kumagai, M. Hasegawa, S. Miyanari, Y. Sugawa, Y. Sato, T. Hori, S. Ueda, H. Kamiyama and S. Miyano, *Tetrahedron Lett.*, 1997, **38**, 3971–3972.

2 For selected books on calixarenes and their applications, see: (*a*) C. D. Gutsche, *Calixarenes Revisited*, Royal Society of Chemistry, Cambridge, UK, 1998; (*b*) C. D. Gutsche, *Calixarenes: an Introduction*, RSC Publishing, Cambridge, UK, 2nd edn, 2008; (*c*) L. Mandolini and R. Ungaro, *Calixarenes in Action*, World Scientific Publishing Company, 2000; (*d*) P. Neri, J. L. Sessler and M. X. Wang, *Calixarenes and beyond*, Springer Cham, 2016.

3 For selected reviews on thiacalixarenes, see: (*a*) R. Kumar, Y. O. Lee, V. Bhalla, M. Kumar and J. S. Kim, *Chem. Soc. Rev.*, 2014, **43**, 4824–4870; (*b*) P. Lhoták, *Eur. J. Org Chem.*, 2004, **2004**, 1675–1692; (*c*) N. Morohashi, F. Narumi, N. Iki, T. Hattori and S. Miyano, *Chem. Rev.*, 2006, **106**, 5291–5316.

4 (*a*) N. Iki, H. Kumagai, N. Morohashi, K. Ejima, M. Hasegawa, S. Miyanari and S. Miyano, *Tetrahedron Lett.*, 1998, **39**, 7559–7562; (*b*) N. Morohashi, N. Iki, C. Kabuto and S. Miyano, *Tetrahedron Lett.*, 2000, **41**, 2933–2937; (*c*) N. Morohashi, H. Katagiri, N. Iki, Y. Yamane, C. Kabuto, T. Hattori and S. Miyano, *J. Org. Chem.*, 2003, **68**, 2324–2333; (*d*) J. Miksatko, V. Eigner, H. Dvorakova and P. Lhotak, *Tetrahedron Lett.*, 2016, **57**, 3781–3784.

5 N. Iki and S. Miyano, *J. Inclusion Phenom. Macrocyclic Chem.*, 2001, **41**, 99–105.

6 For selected examples of spirodienone route to derivatization of classical calixarenes see: (*a*) A. M. Litwak and S. E. Biali, *J. Org. Chem.*, 1992, **57**, 1943–1945; (*b*) S. Simaan, K. Agbaria and S. E. Biali, *J. Org. Chem.*, 2002, **67**, 6136–6142; (*c*) S. E. Biali, *Synlett*, 2003, **2003**, 0001–0011.

7 (*a*) K. Agbaria and S. E. Biali, *J. Am. Chem. Soc.*, 2001, **123**, 12495–12503; (*b*) S. Thulasi, A. Savithri and R. L. Varma, *Supramol. Chem.*, 2011, **23**, 501–508.

8 A. M. Litwak, F. Grynszpan, O. Aleksiuk, S. Cohen and S. E. Biali, *J. Org. Chem.*, 1993, **58**, 393–402.

9 N. Morohashi, M. Kojima, A. Suzuki and Y. Ohba, *Heterocycl. Commun.*, 2005, **11**, 249–254.

10 K. Polivkova, M. Simanova, J. Budka, P. Curinova, I. Cisarova and P. Lhotak, *Tetrahedron Lett.*, 2009, **50**, 6347–6350.

11 (*a*) L. Vrzal, M. Kratochvilova-Simanova, T. Landovsky, K. Polivkova, J. Budka, H. Dvorakova and P. Lhotak, *Org. Biomol. Chem.*, 2015, **13**, 9610–9618; (*b*) T. Landovsky, M. Tichotova, L. Vrzal, J. Budka, V. Eigner, H. Dvorakova and P. Lhotak, *Tetrahedron*, 2018, **74**, 902–907.

12 T. Landovsky, H. Dvorakova, V. Eigner, M. Babor, M. Krupicka, M. Kohout and P. Lhotak, *New J. Chem.*, 2018, **42**, 20074–20086.

13 N. Broftová, T. Landovský, H. Dvořáková, V. Eigner, M. Krupička and P. Lhoták, *Org. Biomol. Chem.*, 2023, **21**, 4620–4630.

14 T. Landovsky, V. Eigner, M. Babor, M. Tichotova, H. Dvorakova and P. Lhotak, *Chem. Commun.*, 2020, **56**, 78–81.

15 T. Landovsky, M. Babor, J. Cejka, V. Eigner, H. Dvorakova, M. Krupicka and P. Lhotak, *Org. Biomol. Chem.*, 2021, **19**, 8075–8085.

16 D. R. Williams and L. Fu, *Org. Lett.*, 2010, **12**, 808–811.

17 (*a*) C. Bannwarth, E. Caldeweyher, S. Ehlert, A. Hansen, P. Pracht, J. Seibert, S. Spicher and S. Grimme, *Wiley Interdiscip. Rev.: Comput. Mol. Sci.*, 2021, **11**, e1493; (*b*) C. Bannwarth, S. Ehlert and S. Grimme, *J. Chem. Theory Comput.*, 2019, **15**, 1652–1671.

18 (*a*) L. A. Flippin, D. S. Carter and N. J. P. Dubree, *Tetrahedron Lett.*, 1993, **34**, 3255–3258; (*b*) S. El Rayes, A. Linden, K. Abou-Hadeed and H.-J. Hansen, *Helv. Chim. Acta*, 2010, **93**, 1894–1911.

19 S. C. Farmer and S. H. Berg, *Molecules*, 2008, **13**, 1345–1352.

20 (*a*) T. Y. Yu, Z. J. Zheng, J. H. Bai, H. Fang and H. Wei, *Adv. Synth. Catal.*, 2019, **361**, 2020–2024; (*b*) F. Takahashi, K. Nogi and H. Yorimitsu, *Org. Lett.*, 2018, **20**, 6601–6605.

21 (*a*) H. Gilman and D. R. Swayampati, *J. Am. Chem. Soc.*, 1955, **77**, 3387–3389; (*b*) T. Kimura, Y. Horie, S. Ogawa, N. Furukawa and F. Iwasaki, *Heteroat. Chem.*, 1993, **4**, 243–252; (*c*) T. Kimura, Y. Ishikawa, K. Ueki, Y. Horie and N. Furukawa, *J. Org. Chem.*, 1994, **59**, 7117–7124.

22 J. Miksatko, V. Eigner and P. Lhotak, *RSC Adv.*, 2017, **7**, 53407–53414.

23 F. Neese, *Wiley Interdiscip. Rev.: Comput. Mol. Sci.*, 2012, **2**, 73–78.

24 S. Ehlert, M. Stahn, S. Spicher and S. Grimme, *J. Chem. Theory Comput.*, 2021, **17**, 4250–4261.

25 Bruker, *APEX4, SAINT and SADABS*, Bruker AXS Inc., Madison, Wisconsin, USA, 2021.

26 L. Palatinus and G. Chapuis, *J. Appl. Crystallogr.*, 2007, **40**, 786–790.

27 P. Betteridge, J. Carruthers, R. Cooper, K. Prout and D. Watkin, *J. Appl. Crystallogr.*, 2003, **36**, 1487.

28 J. Rohlicek and M. Husak, *J. Appl. Crystallogr.*, 2007, **40**, 600–601.

29 A. Altomare, G. Cascarano, C. Giacovazzo, A. Guagliardi, M. C. Burla, G. Polidori and M. Camalli, *J. Appl. Crystallogr.*, 1994, **27**, 435.